SAE INTERNATIONAL

ARTICLE INFO
Article ID: 01-11-01-0002
Published: 11 May 2018

doi:10.4271/01-11-01-0002

Exploring the Potential of Combustion on Titan

Christopher Depcik, University of Kansas

Abstract

Significant attention has been focused on Mars due to its relative proximity and possibility of sustaining human life. However, its lack of in-situ sources of energy presents a challenge to generate needed energy on the surface. Comparatively, Titan has a nearly endless source of fuel in its atmosphere and lakes, but both are lacking in regards to their oxidizing capacity. The finding of a possible underground liquid ammonia-water lake on Titan suggests that oxygen might actually be within reach. This effort provides the first theoretical study involving a primary energy generation system on Titan using the atmosphere as a fuel and underground water as the source for the oxygen via electrolysis from wind generated electricity. Thermodynamic calculations and use of chemical kinetics in a zero-dimensional Homogeneous Charge Compression Ignition (HCCI) engine model demonstrate that is indeed possible to operate an internal combustion engine on the surface of Titan while providing heat for terraforming and human activities. Subsequent terraforming estimates illustrate that while the potential for energy and heat exists, the amount of needed hardware is largely impractical. However, the findings may stimulate further curiosity by others to look towards outer space and imagine what might be possible.

History

Received: 30 Sep 2017
Revised: 02 Jan 2018
Accepted: 03 Jan 2018
e-Available: 07 Apr 2018

Keywords

Titan, Solar System, Combustion, Terraforming, Chemical Kinetics, Energy

Citation

Depcik, C., "Exploring the Potential of Combustion on Titan," *SAE Int. J. Aerosp.* 11(1):2018, doi: 10.4271/01-11-01-0002.

ISSN: 1946-3855
e-ISSN: 1946-3901

Introduction

As humans continue to influence the environment, it is conceivable that we may eventually reach a planetary-scale tipping point beyond which it is not possible to recover [1, 2]. This is particularly troublesome given the absence of habitable planets in the solar system to which life could migrate. Currently, there is discussion regarding the possibility of terraforming Mars for human life [3]. Key issues to this happening are its lack of atmosphere and relatively cold surface temperature as illustrated in Table 1 [4, 5, 6, 7, 8, 9, 10, 11, 12, 13, 14, 15]. Investigating the requirements for carbon dioxide (CO_2), nitrogen (N_2), and water (H_2O), it appears that it is indeed possible to artificially produce an atmosphere to sustain life [13, 16]. One speculative option to warm the surface is to introduce chloroflurocarbons (CFCs in Table 2 [17, 18, 19, 20, 21, 22]) into the atmosphere to generate the needed greenhouse effect [23]. While transporting sufficient raw materials from earth is not feasible, it does appear that enough chlorine (Cl), fluorine (F), and bromine (Br) may be available to manufacture 3×10^{12} tons of CFCs needed each year to offset ultraviolet photolysis losses [13]. However, a significant amount of energy is needed to produce these CFCs on the planet's surface while also supporting terraforming endeavors.

James et al. indicates that the most effective approach for generating energy on the surface of Mars is to couple solar dynamic, photovoltaic, wind, nuclear, and even conventional internal combustion (IC) engine technologies to energy storage devices [24]. Given the magnitude of energy required to support human activities (e.g., on Earth this is currently around 18 terawatts) and synthesize the level of CFCs needed, both solar and wind energy technologies would need massive installations due to their relatively diffuse energy production capabilities. Moreover, NASA has additionally stated that the thin atmosphere of Mars makes it difficult to generate energy from wind; hence,

TABLE 1 Comparison of Earth, Mars, and Titan properties.

	Earth	Mars	Titan
Radius [km]	6378	3394	2575
Surface area [km^2]	5.11×10^8	1.45×10^8	8.30×10^7
Average density [kg/m^3]	5500	3950	1880
Total mass [kg]	6.0×10^{24}	6.5×10^{23}	1.345×10^{23}
Escape velocity [km/s]	11.2	5.0	2.639
Surface gravity [m/s^2]	9.8 (1 g)	3.7 (0.38 g)	1.352 (0.14 g)
Average surface temperature	+15°C	−60°C	−179°C (94 K)
Temperature range	−60 to +50°C	−145 to +20°C	+/−5 K
Surface pressure [kPa]	101.3	0.5-1	147
Mean distance from sun [km]	1.49×10^8	2.28×10^8	1.428×10^9
Orbital eccentricity	0.0167	0.0934	0.0288
Rotation rate [hrs]	24.0	24.62	382.67
Year [days]	365.25	686.98	10759
Obliquity	25.19°	23.45°	0.3°
Average sunlight reaching planet [W/m^2]	345	147	~0.5-3.5
Atmospheric composition [% vol]			
N_2	78	2.7	94-98
O_2	21	0.13	
CO_2	0.038	95.3	
Ar	0.93	1.6	
CO	10^{-5}	0.07	
CH_4	1.7×10^{-4}		2-6
H_2	0.5×10^{-4}		0.1-0.4
H_2O	0.1-3		

extremely high altitudes are required with dust storms potentially providing the only avenue for significant energy generation [25]. Nuclear is definitely an option on Mars [26, 27] (and Titan [28]) with space power sources proving to be safe and reliable [29]. With respect to IC engines, the lack of accessible fuel on Mars reduces its possibility although utilizing the Leidenfrost effect to create dry ice engines using spinning disks of available CO_2 embedded with magnets is not out of the realm of possibilities [30, 31]. Furthermore, previous NASA research illustrates the possibility of running IC engines on Mars using a mixture of synthesized methane, carbon dioxide, and oxygen [32] potentially to power aircraft [33] or surface vehicles [34].

TABLE 2 Select species potentially used for generating a greenhouse effect.

Species	Ozone depletion potential	Global warming potential	Atmospheric lifetime
CF_3Br	10	7140	65
C_2F_6	0	12200	10,000
CF_3Cl	1	14420	640
CF_2Cl_2	1	10900	100
N_2O	0.017	298	114
CH_4	Likely negative	25	12
CO_2	0	1	NA

In comparison, Saturn's largest moon Titan has ample hydrocarbon resources in its atmosphere and lakes, but unfortunately no free oxygen [35]. The level of energy available is potentially hundreds of times more than Earth's oil and natural gas reserves [36]. Furthermore, while Titan is considerably farther away from the sun than Mars with dramatically less solar insolation at the surface [9], it may still be within (9.54 AU) the limits of sustaining life (100 AU) [35]. Given its relative coldness (Table 1), McKay estimates that it is unlikely that Earth-like life could exist [35] with researchers stating that it may take a few billion years before this possibility when the Sun becomes a red giant and heats the outer solar system [37]. One hypothetical option to increase surface temperatures could involve placing large mirrors in orbit to concentrate solar energy; e.g., Mars surface temperature would increase by 2% using a mirror approximately 10^{12} m^2 in size [13]. Another theoretical option would be to follow a similar approach to Mars and generate high global warming potential CFCs using the hydrocarbon resources available on the planet. Currently, no information can be found for Cl, F, and Br resources on Titan; however, the possibility of using combustion for power on Titan is intriguing and warrants further examination. Furthermore, unlike nuclear power, combustion could actually be used to terraform the atmosphere while generating useful power and heat. Assuming a troposphere height of 6.6 km [38], a perfectly spherical moon, and an atmosphere consisting of 5.65% CH_4, 94.24%, N_2, and 0.11% H_2 [38, 39], approximately 9.398×10^{16} kg and 2.304×10^{14} kg of CH_4 and H_2, respectively, are available that can be used as fuels.

As a result, this paper explores a theoretical combustion system on Titan using mass, energy, and entropy balances. Wind energy is used to electrolyze a subsurface liquid ocean (discussed in the next section) to provide the needed oxygen for combustion and terraforming the atmosphere. Through combustion of Titan's atmosphere, H_2O can be generated at the surface removing atmospheric CH_4 while recovering power and heat for use elsewhere. One significant assumption employed in the model presented is that heat transfer to the ambient is largely neglected. Because this is the first paper investigating combustion on Titan, the calculations provided will indicate an upper bound on an estimate. In order to begin the appraisal, the first item to cover includes the flow rates of hydrogen, oxygen, and nitrogen from electrolysis.

Subsurface Ocean Electrolysis

Utilizing the hydrocarbons through combustion on Titan will require oxygen. Based on theoretical models of Titan's formation and evolution along with Cassini radar observations and Schumann resonance data, researchers have indicated that there may be a subsurface ammonia-water ocean [40, 41, 42, 43, 44, 45, 46, 47, 48] with ammonia in concentrations between 5% and 15% [42, 43, 49, 50]. An ice shell that may be 20-50 km thick at certain locations overlies this ocean [41, 45, 51, 52, 53]. While this is significantly deeper than the deepest manmade borehole on Earth (Kola Superdeep at 12.2 km), drilling on Titan may not encounter the same subsurface heat issues that can negatively influence the boring operation. This is because the core of Titan is colder than Earth;

Titan's core temperature is thought to be around 900 K [41] with Earth's core temperature estimated to be 4850 K [54]. Furthermore, since the subsurface ammonia-water ocean on Titan has been estimated to be at 24 MPa [53], this is lower than observed bottomhole pressures for oil drilling activities on Earth that can reach up to 90 MPa [55]. Hence, while it would be costly to reach this ocean, it is not out of theoretical reach.

Therefore, both fuel and oxygen (from water in the subsurface ocean) are theoretically within reach on Titan. Moreover, the greater atmospheric density of Titan makes wind-powered electrolysis of the subsurface ocean to recover its oxygen a possibility. Whereas a 30 m/s Martian wind will provide the same power as a 6 m/s wind on Earth [56], only about a 4 m/s Titan wind is needed generate the same amount of power. With regards to wind potential, Porco et al.'s tracking of cloud motions on Titan found easterly winds with speeds as high as 34 m/s [57]. There were definite zones of wind [58] and at an altitude of 30 km, wind speed was found to be about 10 m/s. Nearer to the surface (lowest 5 km), wind speeds were the lowest at around 1.4 m/s [59]. In addition, the low gravity on Titan would reduce the load on the blades of wind turbines [60] allowing for taller wind turbines with longer blades than on Earth (e.g., without gravity, internal loads on the gearbox are significantly reduced [61]). Future efforts should study the impact of gravity, air friction, and other wind turbine parameters for Titan (similar to [62] for Mars) while also considering the materials needed to construct a wind turbine using additive manufacturing on the surface. This can be accomplished through the development of a wind turbine model using zonal wind estimations [63] while employing the Titan Wind Tunnel [64] for experimental measurements of scale models.

It is important to note that the absence of a subsurface ocean is still compatible with other models of Titan's interior [41]. However, based on modeling studies of Titan, it has been estimated that the ocean temperature is 250 K at 240 bars of pressure [53] and Schumann-like resonance indicates a liquid structure [65]. For this paper, it is assumed that a subsurface ocean exists at a 15% ammonia concentration by mass with water (15.73% ammonia by volume) as this predicts a liquid phase at these conditions [66]. Since ammonia is a relatively significant fraction of this ocean, electrolysis of the mixture may result in a mixture of species leaving the anode. This is because liquid ammonia electrolysis results the molar fractions of ½ N_2 (anode) and 3/2 H_2 (cathode); whereas, water electrolysis results in the molar fractions of ½ O_2 (anode) and H_2 (cathode) [67]. Investigating the literature regarding the electrolysis of ammonia-water solutions only finds contact "glow-discharge" papers where the anode is placed a predetermined distance above the liquid surface (anode is platinum wire, cathode is small sheet of platinum foil) [68, 69, 70, 71]. Hence, in the absence of specific information, it will be assumed that the molar balance of electrolysis is as follows (α = 0.84269, β = 0.15731):

$$\alpha H_2O + \beta NH_3 \rightarrow eH_2 + fO_2 + gN_2 \qquad \text{Eq. (1)}$$

Pure hydrogen will leave the cathode and a mixture of oxygen and nitrogen will emanate from the anode with all species having the same pressure and temperature [72]. It is possible to remove ammonia from the water using air stripping and other technologies prior to electrolysis [73]. However, this will add complexity while being inefficient at the extremely low temperatures of the Titan environment (e.g., efficiency degrades for air stripping from 90-95% to 75% as temperature drops from 293 K to 283 K [74]).

From the first law of thermodynamics, the thermoneutral cell potential of electrolysis (E_{tcp}) in volts can be determined [67, 72, 75, 76, 77]:

$$E_{tcp} = \frac{\dot{W} - \dot{Q}}{nF} = \frac{\dot{n}_{H_2O}\bar{h}_{H_2O} + \dot{n}_{NH_3}\bar{h}_{NH_3} - \dot{n}_{H_2}\bar{h}_{H_2} - \dot{n}_{N_2}\bar{h}_{N_2} - \dot{n}_{O_2}\bar{h}_{O_2}}{nF} \qquad \text{Eq. (2)}$$

However, most researchers use the reversible cell potential (E_{rev}) incorporating the second law in electrolysis calculations because $T\Delta S$ can be provided from the environment at a temperature T:

$$E_{rev} = \frac{\dot{W}_{rev}}{nF} = \frac{\dot{n}_{H_2O}\bar{g}_{H_2O} + \dot{n}_{NH_3}\bar{g}_{NH_3} - \dot{n}_{H_2}\bar{g}_{H_2} - \dot{n}_{N_2}\bar{g}_{N_2} - \dot{n}_{O_2}\bar{g}_{O_2}}{nF} \qquad \text{Eq. (3)}$$

TABLE 3 Thermoneutral and reversible cell potential calculations.

Pres [MPa]	Temp [K]	Fluid	E_{tcp} [V]	Lit	E_{rev} [V]	Lit	MJ per mole
0.10132	298.15	Water	1.4812	1.481	1.2289	1.229	0.2371
10.132	298.15	Water	1.4789	1.479 1.481	1.3171	1.317 1.319	0.2542
70	523	Water	1.4448	1.443	1.2717	1.275	0.2454
1.015	298.15	NH_3	0.2321	N/A	0.0775	0.077	0.0224
24	250	NH_3	0.2331	N/A	0.1476	N/A	0.0427
24	250	Titan Ocean	1.2205	N/A	1.0997	N/A	0.2289

For standard water and ammonia electrolysis, n is equal to 2 and 3, respectively. Based on the molar balance in Equation 1, the number of electrons for the ammonia/water lake is calculated as:

$$n = 2\alpha + 3\beta \quad \text{Eq. (4)}$$

After adjusting the datum between the liquids and gases while using the ammonia heat and entropy of formation information from [67], the NIST REFPROP database [78] was employed to determine the cell potentials in Table 3 to validate the calculations against the literature. The energy required per mole of liquid ($\bar{Q}_{liq}$) calculation using the reversible cell potential was compared to [67]: 0.0224 MJ/mol$_{NH3}$ equals 7.41 MJ/kg$_{H2}$ with Hanada et al. stating the value as 7.4 MJ/kg$_{H2}$. The molar flow rate of ocean that can be converted by wind power ($\dot{W}_{wind}$) is then calculated,

$$\dot{n}_{ocean} = \frac{\dot{W}_{wind}}{\bar{Q}_{liq}} \quad \text{Eq. (5)}$$

subsequently leading to the molar flow rates of H_2, O_2, and N_2 using the balance in Equation 1. In addition to the combustion studies presented in this paper, the calculations in this section can be employed for other Titan terraforming efforts since H_2 is a valuable reactant for chemicals and as a rocket fuel [79, 80]; whereas, O_2 and N_2 are needed for settlements [81].

Flow to Engine

Ideally, it would be best to build the lightest, simplest, and most efficient/powerful engine given transportation costs to Titan. This is estimated to be $7330/kg using the SpaceX Falcon Heavy at a launch cost of $90M with a scaled payload of 12277 kg to Titan based on the reported payloads to Mars and Pluto [82, 83]. Moreover, a simple engine would minimize the required materials for on-site construction using additive manufacturing (e.g., [84]) potentially employing iron from the rocky core of Titan [85] assuming drilling technology is sufficient to penetrate and extract needed elements. This engine is postulated here to be an air-cooled compression ignition (CI) engine running on spontaneous auto-ignition (i.e., homogeneous charge compression ignition - HCCI [86]). However, to use either the atmosphere or lakes as a fuel will require a heated intake. Since these mixtures and the oxygen coming from the ocean are relatively cold, auto-ignition will be difficult to achieve. Because the literature demonstrates that adding H_2 in a dual-fuel manner can be beneficial due to its lower ignition energy in comparison to methane [87, 88], it may be advantageous to allow some of the hydrogen from electrolysis to travel along with the oxygen. Moreover, adding hydrogen to methane improves HCCI combustion stability [89, 90] because it provides a source of H atoms, subsequently augmenting the $H + O_2 \Leftrightarrow OH + O$ combustion reaction promoting easier ignition [91, 92]. Furthermore, there may be enough exhaust energy available to heat the intake. As a

result, Figure 1 (in Appendix) demonstrates the potential pathway of flow to the engine while using exhaust to heat the intake. It does allow for a variable amount of H_2 to mix (1-q by volume) with the N_2 and O_2 coming from the anode.

All components in Figure 1 are evaluated according to the first and second laws of thermodynamics, respectively, on a rate basis assuming that these laws hold true to Titan (e.g., Titan atmospheric kinetics have been simulated using conventional thermodynamic constraints [93]):

$$\frac{dU}{dt} = \dot{Q} - \dot{W} + \sum_{in} \dot{m}h - \sum_{out} \dot{m}h \qquad \text{Eq. (6)}$$

$$\frac{dS}{dt} = \frac{\dot{Q}}{T_{sur}} + \sum_{in} \dot{m}s - \sum_{out} \dot{m}s + \dot{\sigma} \qquad \text{Eq. (7)}$$

A steady state model is assumed eliminating the left hand sides of Equations 6 and 7 with the expansion valve and intake assumed to be adiabatic for simplicity. CHEMKIN curve-fits of the thermodynamics properties are included in order to account for mixture compositions [94].

The process where some H_2 is allowed to remix with N_2/O_2 is assumed to occur at a constant pressure and temperature; hence, due to the entropy of mixing, heat is transferred to the surroundings. Since the ambient is at 147 kPa, this mixture is expanded through an expansion valve or a turbine prior to entering the engine intake. Expansion valves are cheaper, smaller, and would weigh less; whereas, turbines could be used to recover some energy due to the relatively high pressure of the subsurface ocean. In the intake, this $N_2/O_2/H_2$ stream mixes with the Titan atmosphere and is subsequently heated in a perfect heat exchanger (no mixing of streams) using the available energy from the engine exhaust. Using Equation 6, the analysis of this heat exchanger simplifies to the calculations of enthalpy entering and exiting. Here, an assumption is that ample heat energy exists via nuclear or electrical resistance (via wind power) to cold start the engine prior to steady-state operation.

Another method to raise the beginning charge temperature at the start of the compression stroke is to mix a portion of the exhaust directly with the intake (i.e., Exhaust Gas Recirculation - EGR) [89, 95, 96, 97, 98, 99, 100]. The radicals that are part of EGR may aid in the initiation of the HCCI process helping to reduce auto-ignition temperatures [101]. However, too much EGR can prevent combustion from occurring due to its inert nature and this method would preclude the full amount of exhaust energy to be utilized. Furthermore, incorporating an EGR system would add complexity to the setup; whereas, as stated prior, simplicity is preferred given logistical constraints.

The question then becomes what to accomplish with the remaining H_2 from electrolysis. Since Titan's atmosphere has too much nitrogen posing an asphyxiation hazard and ammonia can be used as a fuel for an internal combustion engine [102], Figure 1 illustrates the conversion of atmospheric N_2 into ammonia. Moreover, it may be desired to have a liquid cooled engine to help with energy recovery [103]; hence, instead of using traditional ethylene glycol, liquid ammonia could be used as the engine coolant similar to the International Space Station [104]. Furthermore, Miyahara demonstrates that the rocket fuel hydrazine can be synthesized from mixtures of H_2/N_2 or CH_4/N_2 providing for another avenue of usage [105]. As a result, two additional fuels can potentially be generated on the surface of Titan using the H_2 emanating from electrolysis.

Combustion Reactions and Modeling

Stoichiometric combustion with the atmosphere at the surface (estimated as a = 94.24%, b = 5.65%, c = 0.11% [38, 39]),

$$\left(aN_2 + bCH_4 + cH_2\right) + x\left(zH_2 + fO_2 + gN_2\right) \rightarrow kCO_2 + iH_2O + jN_2 \qquad \text{Eq. (8)}$$

was assumed. While it is known that optimum combustion temperatures and power will be achieved slightly rich [106], stoichiometry is relatively easy to determine. Then, using the calculated molar flow rate of the ocean from Equation 5, the atmospheric species molar flow rates can be found. Since the temperatures and pressures are known for the species entering the heated intake, their combined enthalpy and entropy can be determined. At this point, an iterative procedure is required in order to determine the temperature after the heated intake, which is also assumed for simplicity as the Intake Valve Closing (IVC) temperature. Of note, converting CH_4 to CO_2 in the atmosphere will reduce the current greenhouse effect on Titan (see Table 2); however, if CFCs can be generated in sufficient quantities, they could more than make up for the difference.

TABLE 4 Internal combustion engine parameters.

Variable	SI value	British value
Combustion factor	200 K	360°F
Compression ratio [−]	21.2	
Bore	0.086 m	3.39 in
Stroke	0.075 m	2.95 in
Connecting rod length	0.11842 m	4.662 in
Cylinder head surface area	0.005809 m	9.004 in^2
Piston head surface area	0.005809 m	9.004 in^2
Intake valve closing [deg BTDC]	122	
Exhaust valve opening [deg ATDC]	144	
Wall temperature	400 K	260°F
Engine speed [rpm]	3600	
Volumetric efficiency [%]	85	

Since the engine will be required to run in HCCI mode and is dependent on chemical kinetics to operate, a simple thermodynamic analysis is not possible. Moreover, because this effort is postulating combustion using a unique fuel, it is pertinent to run kinetic studies to determine if combustion can actually happen. Therefore, a single-zone model employing chemical kinetics was incorporated [107]. For simplicity, the model ignores blow-by past the piston and is only useful from IVC until Exhaust Valve Opening (EVO) when there is not any additional mass entering or exiting. While this omits the engine breathing process along with any internal residual that may result (i.e., internal EGR), trends of operation can still be generated and the overall concept evaluated relatively quickly. The model equations were solved using DVODE [108] while incorporating CHEMKIN to handle the chemical species reactions. In regards to the detailed reaction mechanisms, GRI-Mech 3.0 [109] is often considered to be the standard mechanism for methane combustion and has been shown to correlate well to ignition delay measurements of mixtures of $CH_4/H_2/O_2/N_2$ with upwards of 95% N_2 similar to the Titan atmosphere [110]. Recent efforts in our group [111] finds that the University of California, San Diego (UCSD) propane oxidation mechanism [112] had an overall better accuracy versus a wide number of reaction mechanisms, including GRI-Mech 3.0, with respect to ignition delay calculations. Hence, both the GRI-Mech and UCSD mechanisms were tested. For engine heat transfer, the Hohenberg expression was chosen out of the large number of available convective heat transfer correlations due to its simplicity and relative accuracy while also being used prior when simulating HCCI engines [113, 114].

In order to predict whether combustion is occurring, an assumption of the IVC temperature is first made and the model then simulates a motoring process where the N_2 and O_2 species from the combined intake are the only components sent to the engine. The predicted temperature data are then reviewed to find its maximum, after which the complete intake species (i.e., Equation 8) are used for simulation and the maximum temperature is again reviewed. If this temperature is greater than the maximum motoring temperature by a prescribed amount (combustion factor in Table 4), combustion is said to be occurring. However, peak pressure location for maximum brake torque (MBT) will vary by fuel, engine speed, and load [115]. Hence, even though combustion may be occurring, it may not be happening at the correct crank angle. Therefore, an additional logic switch in the simulation is used to check to make sure that the peak temperature occurs 10° after top dead center for maximum thermal efficiency as estimated by Lavoie et al. [116]. If combustion does not occur, the IVC temperature is increased by 0.1 K and the process is repeated. After a successful iteration, the engine work and heat transfer are calculated and converted into watts using the simulated engine speed that is also utilized to calculate the mass flow rate at IVC:

$$\dot{m}_{\mathrm{IVC}} = \frac{\eta_v \rho_{\mathrm{IVC}} V_d N}{n_R} \qquad \text{Eq. (9)}$$

In other words, the engine speed sets the electrolysis flow rate requirements ($\dot{n}_{ocean}$) in Equation 5. Hence, the simulation iterates on the value of the wind power required in order to run the engine at the required IVC temperature for combustion to occur. Finally, since there is a significant drop in temperature after EVO [117], the ideal exhaust blowdown assumption is used (isentropic expansion of the gas) in order to provide a slightly more realistic value of the exhaust temperature [106]. At this point, the energy and entropy balance for the heated intake can be calculated in order to determine if enough energy exists in the exhaust to provide the needed heating given a perfect heat exchanger.

Because our laboratory employs a high compression ratio, air-cooled CI engine (Table 4) [118], it was used for the simulation efforts as it provides for potential experimental validation. Moreover, as the engine is rated for 3600 rpm and the goal is to generate the maximum power possible, the engine speed was set equal to this value. The wall temperature was set at 400 K with the piston temperature estimated as 100 K hotter based on literature findings [119, 120]. The volumetric efficiency of the engine was set to an average value based on past testing efforts. Obviously, the wall temperature will be a function of the ambient heat transfer and the engine should be in an insulated environment to prevent too much heat loss.

Results and Discussion

In Figure 1, the mass flow rates, pressures, temperatures, species, power used and generated, along with the entropy generation results are provided for an example scenario employing the GRI mechanism when 10% of the hydrogen coming from the ocean is utilized. Investigating the use of a turbine instead of an expansion valve finds that it would generate some power and may be an appropriate addition given the length of time over which terraforming could take place (discussed later). After ignoring ambient heat transfer, it does appear that it is indeed possible to burn the Titan atmosphere for power. In addition, since the exhaust temperature leaving the heat recovery jacket is at 557.9 K, further using this stream for heating an enclosure (or the ambient) is feasible. However, this assumed the engine was possible to start while cold. Hence, future work should analyze the time-dependent thermodynamics of the intake and engine in order to reach the required temperatures for steady-state operation in Figure 1 using heat from a nuclear source or wind-powered electric heater.

Looking at the in-cylinder pressure and temperature plots of Figure 2a and 2b, respectively, shows that the engine may encounter a significantly energetic combustion event. This excessive pressure rise is why HCCI operation is often limited to lower engine loads and EGR is utilized to prevent a dramatic heat release and its associated noise. However, the in-cylinder temperature when using a low amount of electrolysis hydrogen is within engine operating limits. As more hydrogen from the ocean is used, the temperature increases due to the larger energy capacity of hydrogen and the fact that less inert nitrogen is coming from the environment to mitigate the energy release (i.e., atmospheric nitrogen acts as a heat sink). Furthermore, because the ignition energy is lower for hydrogen and it aids in the initiation of combustion, the temperature needed at IVC is reduced. Therefore, while the pressure rise is significant and HCCI combustion stability can be a potential issue, designing an engine to handle this combustion scenario is possible as illustrated by others who have successfully operated HCCI air-cooled engines [121, 122, 123, 124]. Moreover, one could burn later towards EVO to reduce the cylinder pressure. While this would reduce the engine power available, it would also increase the amount of energy sent into the exhaust while lowering engine noise.

In order to determine if there is an optimum usage of electrolysis hydrogen, a parametric study was accomplished with both chemical mechanisms while varying the hydrogen used from 0% to 78%. The maximum H_2 allowed while burning the atmosphere according to the balances of Equations 1 and 8 is 78.125%. Investigating Figure 3 finds an initial steep drop in the required IVC temperature for both mechanisms when a small fraction of hydrogen from the ocean augments the oxygen stream. As discussed prior,

this is because the addition of hydrogen leads to increased H radicals during combustion that play a significant role in accelerating the $H + O_2 \Leftrightarrow OH + O$ chain branching reaction [91, 92]. Furthermore, the relatively large flammability limit of hydrogen helps promote a more combustible mixture when only a small fraction is utilized in comparison to other hydrocarbon fuels [125]. As the amount of H_2 fraction increases, the maximum combustion temperature and associated engine power grows while the IVC temperature continues to fall; however, now more linearly with the UCSD mechanism indicating a more dramatic reduction. This indicates that the UCSD mechanism is more sensitive to changes in H (and potentially O and OH) radicals during the combustion process. Since both mechanisms demonstrated the same trends with hydrogen, only the GRI results will be explained moving forward unless the UCSD results require a further description.

Interestingly, the initial drop of IVC temperature slightly decreased the maximum combustion temperature even as the more energetic H_2 was added. This is because the temperature before combustion (i.e., compression temperature) was lower resulting in a reduced starting point for the combustion process without sufficient H_2 added to make up the difference. This drop in compression temperature can be seen in Figure 2b via the trend at 360° (aka TDC) with IVC temperature. However, since the inlet pressure remains constant, replacing N_2 and CH_4 with hydrogen and its higher ratio of specific heat results in an increase in compression pressure (Figure 2) because pressure has an exponential dependency on this parameter.

By examining the flow rate through the engine in Figure 4, we find that the inflection point of hydrogen's impact on IVC temperature ($1\text{-}q = 0.05$) results in the largest system flow rate. This is because it provides the greatest reduction in energy required to heat the intake while minimizing the hydrogen needed from the ocean. As a result, this inflection point maximizes the conversion of the atmosphere as shown in Figure 5. As more hydrogen is utilized, the temperature grows dramatically stemming largely from the more energetic combustion event (Figure 2b). As can be expected with this increase in hydrogen usage, the exhaust flow rate of water grows as provided in Figure 6. Reflecting the trends of Figures 4 and 5, the maximum generation of CO_2 is found to be at the inflection point as the most CH_4 from the ambient atmosphere is utilized.

Figure 7 explores the system efficiency (power produced by the engine over the wind turbine power), coefficient of performance (exhaust heat available over the net power required, analogous to a heat pump), and total entropy generation of the system. At extremely high hydrogen flow rates, the efficiency drops dramatically and entropy generation grows since the system is simply re-burning what it electrolyzed. There does appear to be a plateau of efficiency starting at the inflection point of hydrogen use and continuing until approximately 40% of the hydrogen generated is re-used for combustion (GRI-Mech maximum efficiency is 39.18% at $q = 0.81$). Even though the wind turbine power required grows linearly in this regime, the engine is seeing a reduced IVC temperature promoting a higher intake density (Equation 9) and more power-dense engine. Of note, the more dramatic reduction in IVC temperature by the UCSD mechanism results in the system efficiency increasing by approximately 2% up to the 35% hydrogen usage point. Using the entire system as a heat pump finds a maximum coefficient of performance of 1.13 at $q = 0.97$ for the GRI-Mech. Overall, it appears that designing for the hydrogen

FIGURE 2 a) In-cylinder pressure and b) temperature versus crank angle as a function of added hydrogen fraction.

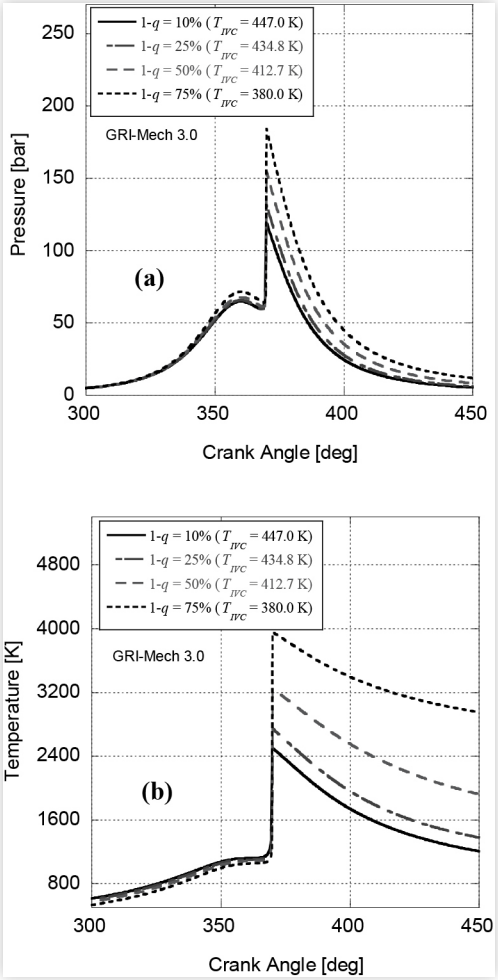

FIGURE 3 Electrolysis H_2 parametric study investigating the required IVC temperature.

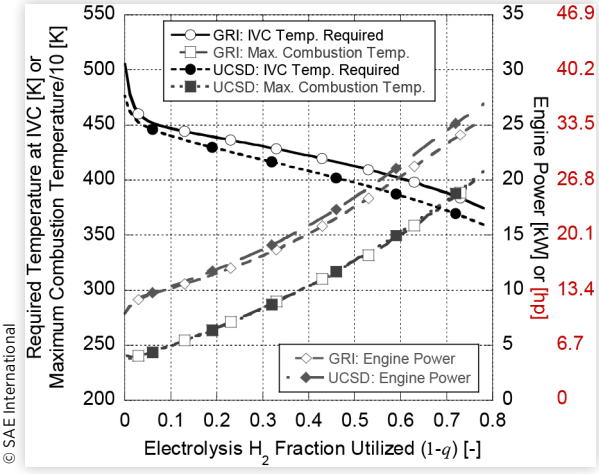

FIGURE 4 Impact of added H_2 (GRI-Mech 3.0) on engine flow rate and exhaust temperature.

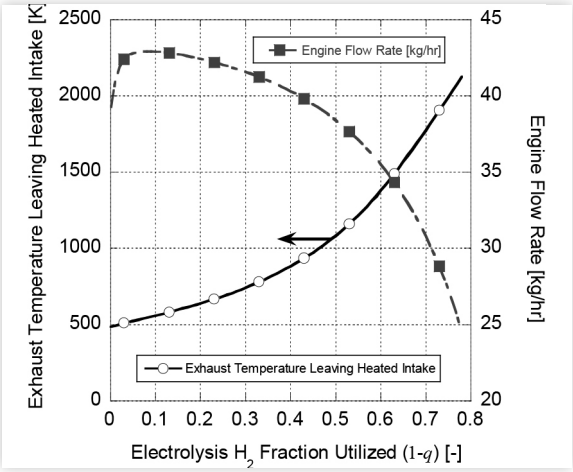

FIGURE 5 Impact of added H_2 (GRI-Mech 3.0) on ocean and ambient flow rates.

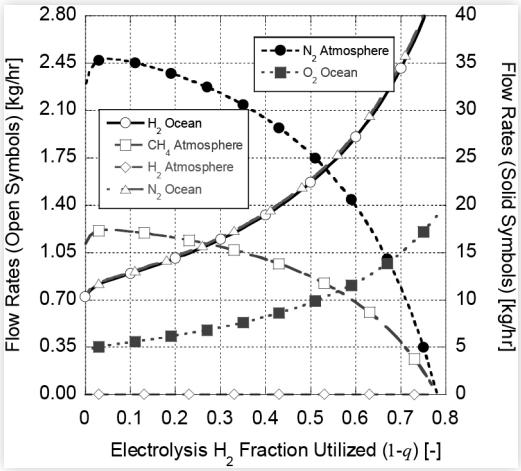

FIGURE 6 Impact of added H_2 (GRI-Mech 3.0) on exhaust flow rates.

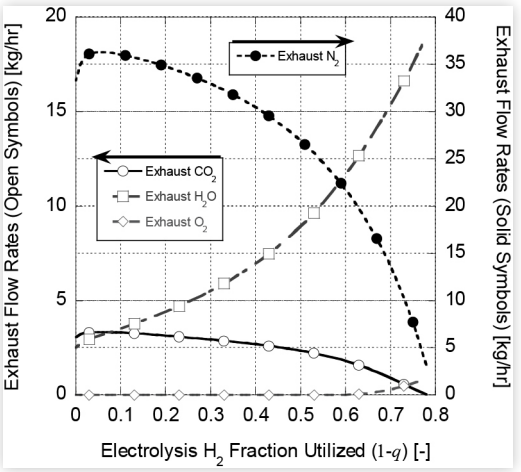

inflection point (q = 0.95) might provide the most beneficial system setup since the efficiency and coefficient of performance are near optimums, 38.59% and 1.12, respectively, and this maximizes the conversion of the atmosphere.

Obviously, it would be significantly more efficient to use the wind turbine to create any needed electrical energy for settlements or terraforming purposes. However, while converting Titan's atmosphere without employing oxygen using direct electrical energy can be accomplished via glow discharge to generate hydrazine [105] and electrical catalyst heating to create ammonia [126] or higher hydrocarbons from methane [127], this requires the selection of a proper catalyst along with a heterogeneous chemical kinetics study. Hence, this is left to future work to contrast against the combustion methodology employed here.

In order to provide an estimate of the scope involved with terraforming Titan, this inflection point was employed to calculate the overall time needed. Given the calculated mass of 9.398×10^{16} kg of CH_4 in the troposphere, the one engine used in this simulation effort would take 8.810×10^{12} years to completely remove all CH_4 and H_2 while generating 7.326×10^8 terawatt-hrs (TWh) of energy. This would require 1.899×10^9 TWh of wind energy and the troposphere (assuming that an added catalyst on the exhaust would ensure complete conversion via Equation 8) chemical profile by volume would equal 4.91% CO_2, 11.26% H_2O, and 83.83% N_2 if it was warm enough to guarantee all CO_2 and H_2O remained in gaseous form. As a check, the first law of thermodynamics (Equation 6) was used to simulate a new troposphere temperature assuming all exhaust heat went into the current troposphere as the atmosphere was converted. It was determined that the troposphere temperature would equal 805.2 K. After this conversion, in order to achieve a breathable oxygen concentration of 19.5% by volume, 9.691×10^{17} kg of O_2 would need to be added from the ocean (while bringing along some N_2) requiring an additional 4.571×10^9 TWh of wind energy. Since this oxygen flow would be at 250 K, the final temperature of the troposphere would be 667.4 K with a chemical profile equal to 3.77% CO_2, 8.65% H_2O, and 68.07% N_2. This would be too much CO_2 for human beings to function, but the fact that there is enough energy in the troposphere to theoretically terraform the planet while providing enough heat to warm the surface is intriguing. Moreover, coupling this activity to a nuclear power source would ensure sufficient heat generation from the beginnings of extraterrestrial base activity. Finally, in order to reduce the time of terraforming to a century, it would take 8.81×10^{10} single cylinder engines or a total engine volume of 3.84×10^{10} L. Hence, bringing engines from Earth would be cost prohibitive with the energy requirements of additive manufacturing on Titan still needing examination. Further work can be done to more rigorously analyze the system in regards to what would make Titan habitable based on the efforts of Beech and Dole [128, 129].

Conclusions

While substantially further away from the sun than Mars, the vast amount of hydrocarbon sources on the surface of Titan make an interesting argument to investigate the possibility of generating power and heat. With this thought in mind, a novel system is proposed where wind energy is used to electrolyze a subsurface ammonia-water liquid

ocean to generate oxygen for combusting the Titan atmosphere. Two chemical kinetic mechanisms are utilized to prove theoretically that it is conceivable to generate power using conventional internal combustion engine technologies through HCCI-enabled combustion. Moreover, the exhaust energy that results is more than sufficient to provide for the required engine inlet heating. Hence, the potential left over exhaust enthalpy could be used for enclosure heating purposes. A parametric study finds that strategic use of some of the hydrogen generated from electrolysis of the underground lake lowers the required engine inlet temperature while maximizing the conversion of the atmosphere. This found inflection point indicates a first-pass optimization of the proposed system and was used to calculate a rough estimate of the requirements to terraform Titan. A significant omission is the impact of ambient heat transfer; however, this effort opens a door for continued exploration into terraforming Titan using readily available technologies. Further discovery can include ammonia and hydrazine generation on the moon to create two additional fuels. Obviously, this paper presents a highly theoretical study, but the outcomes are interesting and might stimulate further curiosity by others to look towards the stars and think about what might be possible.

FIGURE 7 Overall system results as a function of added H_2.

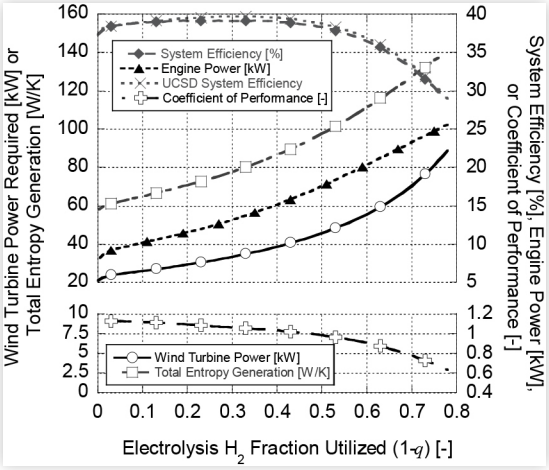

Contact Information

Christopher Depcik,
Associate Professor,
Department of Mechanical Engineering,
depcik@ku.edu,
Ph: 785-864-4151,
3144C Learned Hall, 1530 W. 15th Street
Lawrence, KS, 66045-4709

Nomenclature

a - Atmosphere molar nitrogen balance
b - Atmosphere molar methane balance
c - Atmosphere molar hydrogen balance
e - Molar amount of hydrogen generation from electrolysis
E_{rev} - Reversible cell potential of electrolysis
E_{tcp} - Thermoneutral cell potential of electrolysis
F - Faraday constant (96485 C mol^{-1})
f - Molar amount of oxygen generation from electrolysis
g - Molar amount of nitrogen generation from electrolysis
$\bar{g}$ - Molar Gibbs free energy
h - Mass specific enthalpy
$\bar{h}$ - Molar specific enthalpy
i - Resultant combustion molar amount of water
j - Resultant combustion molar amount of nitrogen
k - Resultant combustion molar amount of carbon dioxide
$\dot{m}$ - Mass flow rate
N - Engine speed
n - Number of electrons transferred per formula conversion
n_R - Four-stroke engine

$\dot{n}$ - Molar flow rate of species or ocean

$\dot{Q}$ - Heat transfer

$\bar{Q}_{liq}$ - Energy required per mole of liquid

s - Mass specific entropy

S - Total entropy

T - Temperature

t - Time

U - Total internal energy

V_d - Displacement volume of engine

$\dot{W}$ - Boundary work

$\dot{W}_{wind}$ - Wind power

x - Stoichiometric combustion balance parameter

z - Molar fraction of hydrogen coming from electrolysis $(1\text{-}q)\times e$

Greek Variables

α - Mole fraction of water in ocean

β - Mole fraction of ammonia in ocean

η_v - Volumetric efficiency

ρ_{IVC} - Density at Intake Valve Closing

$\dot{\sigma}$ - Entropy generation

References

1. Barnosky, A.D., Hadly, E.A., Bascompte, J., Berlow, E.L. et al., "Approaching a State Shift in Earth's Biosphere," *Nature* 486(7401):52-58, 2012, doi:10.1038/nature11018.
2. Barnosky, A.D., Matzke, N., Tomiya, S., Wogan, G.O.U. et al., "Has the Earth's Sixth Mass Extinction Already Arrived?" *Nature* 471(7336):51-57, 2011, doi:10.1038/nature09678.
3. Musk, E., "Making Humans a Multi-Planetary Species," *New Space* 5(2):46-61, 2017, doi:10.1089/space.2017.29009.emu.
4. Zebker, H.A., Stiles, B., Hensley, S., Lorenz, R. et al., "Size and Shape of Saturn's Moon Titan," *Science* 324(5929):921-923, 2009, doi:10.1126/science.1168905.
5. Coustenis, A. and Taylor, F.W., *Titan: The Earth-Like Moon*, (River Edge, World Scientific, 1999), ISBN:9789810239213.
6. Jet Propulsion Laboratory, "Solar System Dynamics Group, Horizons On-Line Ephemeris System," 2015, http://ssd.jpl.nasa.gov/, June 9, 2017.
7. Heintz, A. and Bich, E., "The Atmosphere and Internal Structure of Saturn's Moon Titan, a Thermodynamic Study," in Tadashi, M. (Ed.), *Thermodynamics*, (London, UK, InTech, 2011), doi:10.5772/13108.
8. Bryan, W.S., Randolph, L.K., Ralph, D.L., Scott, H. et al., "Determining Titan's Spin State from Cassini Radar Images," *The Astronomical Journal* 135(5):1669, 2008, doi:10.1088/0004-6256/139/1/311.
9. Lora, J.M., Goodman, P.J., Russell, J.L., and Lunine, J.I., "Insolation in Titan's Troposphere," *Icarus* 216(1):116-119, 2011, doi:10.1016/j.icarus.2011.08.017.
10. Ono, E. and Cuello, J., "Photosynthetically Active Radiation (PAR) on Mars for Advanced Life Support," SAE Technical Paper 2000-01-2427, 2000, doi:10.4271/2000-01-2427.
11. Hempsell, C.M., "Some Speculations on the Construction of Artificial Planets," *Journal of the British Interplanetary Society* 58:392-397, 2005.
12. Graham, J.M., "The Biological Terraforming of Mars: Planetary Ecosynthesis as Ecological Succession on a Global Scale," *Astrobiology* 4(2):168-195, 2004, doi:10.1089/153110704323175133.

13. McKay, C.P. and Marinova, M.M., "The Physics, Biology, and Environmental Ethics of Making Mars Habitable," *Astrobiology* 1(1):89-109, 2001, doi:10.1089/153110701750137477.
14. Bézard, B., Yelle, R.V., and Nixon, C.A., "The Composition of Titan's Atmosphere," in *Titan: Interior, Surface, Atmosphere, and Space Environment*, Edited by Müller-Wodarg, I. et al., (New York: Cambridge Planetary Science, 2014), ISBN:9780511667398.
15. McKay, C.P., "Bringing Life to Mars," *Scientific American Presents* 10(1):52-57, 1999.
16. McKay, C.P., "Requirements and Limits for Life in the Context of Exoplanets," *Proc Natl Acad Sci USA* 111(35):12628-12633, 2014, doi:10.1073/pnas.1304212111.
17. Andersen, S.O. and Madhava Sarma, K., editors, *Protecting the Ozone Layer: The United Nations History*, (New York, Earthscan Publications Ltd., 2012), ISBN:9781849772266.
18. Portmann, R.W., Daniel, J.S., and Ravishankara, A.R., "Stratospheric Ozone Depletion due to Nitrous Oxide: Influences of Other Gases," *Philosophial Transactions of the Royal Society B* 367(1593):1256-1264, 2012, doi:10.1098/rstb.2011.0377.
19. Winterton, N., *Chemistry for Sustainable Technologies: A Foundation*, (Cambridge, The Royal Society of Chemistry, 2011), ISBN:987-1-84755-813-8.
20. Mühle, J., Ganesan, A.L., Miller, B.R., Salameh, P.K. et al., "Perfluorocarbons in the Global Atmosphere: Tetrafluoromethane, Hexafluoroethane, and Octafluoropropane," *Atmos. Chem. Phys.* 10(11):5145-5164, 2010, doi:10.5194/acp-10-5145-2010.
21. Burkholder, J.B., Wilson, R.R., Gierczak, T., Talukdar, R. et al., "Atmospheric Fate of CF_3Br, CF_2Br_2, CF_2ClBr, and CF_2BrCF_2Br," *Journal of Geophysical Research: Atmospheres* 96(D3):5025-5043, 1991, doi:10.1029/90jd02735.
22. Ravishankara, A.R., Daniel, J.S., and Portmann, R.W., "Nitrous Oxide (N_2O): The Dominant Ozone-Depleting Substance Emitted in the 21st Century," *Science* 326(5949):123-125, 2009, doi:10.1126/science.1176985.
23. Lovelock, J.E. and Allaby, M., *The Greening of Mars*, (New York, Warner Books, 1984), ISBN:9780446329675.
24. James, G., Chamitoff, G., and Barker, D., "Resource Utilization and Site Selection for a Self-Sufficient Martian Outpost," NASA Scientific and Technical Information Program Office (NASA/TM-98-206538), 1998.
25. National Aeronautics and Space Administration, "Antarctic/Alaska-Like Wind Turbines Could Be Used on Mars," 2001, http://www.nasa.gov/centers/ames/news/releases/2001/01_72AR.html, June 2, 2016.
26. Hoffman, S.J. and Kaplan, D.I., *Human Exploration of Mars: The Reference Mission of the NASA Mars Exploration Study Team*, NASA Report # NASA-SP-6107, Science Applications International Corporation, Houston, TX, 1997.
27. Fogg, M.J., *Terraforming: Engineering Planetary Environments*, (Warrendale, Society of Automotive Engineers, 1995), ISBN:9781560916093.
28. Hendrix, A.R. and Yung, Y.L., "Energy Options for Future Humans on Titan," *Astrobiol Outreach* 5(2):2332-2519, 2017, doi:10.4172/2332-2519.1000157.
29. Bennett, G.L., "Space Nuclear Power: Opening the Final Frontier," Paper read at *4th International Energy Conversion Engineering Conference and Exhibit*, San Diego, CA, 2006, doi:10.2514/6.2006-4191.
30. Abrams, M., "Dry Ice Power," 2015, https://www.asme.org/engineering-topics-retired/articles/energy/dry-ice-power, accessed February 6, 2016.
31. Wells, G.G., Ledesma-Aguilar, R., McHale, G., and Sefiane, K., "A Sublimation Heat Engine," *Nature Communications* 6:6390, 2015, doi:10.1038/ncomms7390.
32. Bui, H., Coletta, C., and Debois, A., "Mars Methane Engine," National Aeronautics and Space Administration, NASA-CR-197205, 1994.
33. Colozza, A.J., "Comparison of Mars Aircraft Propulsion Systems," National Aeronautics and Space Administration, NASA CR-2003-212350, 2003.
34. Zubrin, R., Baker, D., and Gwynne, O, "Mars Direct - A Simple, Robust, and Cost Effective Architecture for the Space Exploration Initiative," *29th Aerospace Sciences Meeting*, American Institute of Aeronautics and Astronautics, Reno, NV, 1991, doi:10.2514/6.1991-329.

35. McKay, C.P. and Davis, W.L. "Chapter 10 - Astrobiology," in *Encyclopedia of the Solar System*, Third Edition, Edited by Spohn, T., Breuer, D., and Johnson, T.V., (Boston, Elsevier, 2014), 209-231, ISBN:9780124160347.
36. Martinez, C., "Titan's Surface Organics Surpass Oil Reserves on Earth," National Aeronautics and Space Administration, 2008, http://www.nasa.gov/mission_pages/cassini/media/cassini-20080213.html, accessed May 31, 2016.
37. Howard, J., "Polar Winds on Saturn's Moon Titan Makes It More Earth-Like Than Previously Thought," *The Huffington Post*, 2015, http://www.huffingtonpost.com/2015/06/21/polar-wind-titan-earth-like_n_7622606.html, accessed December 6, 2017.
38. Niemann, H.B., Atreya, S.K., Demick, J.E., Gautier, D. et al., "Composition of Titan's Lower Atmosphere and Simple Surface Volatiles as Measured by the Cassini-Huygens Probe Gas Chromatograph Mass Spectrometer Experiment," *Journal of Geophysical Research: Planets* 115(E12):12006, 2010, doi:10.1029/2010je003659.
39. Tan, S.P., Kargel, J.S., Jennings, D.E., Mastrogiuseppe, M. et al., "Titan's Liquids: Exotic Behavior and Its Implications on Global Fluid Circulation," *Icarus* 250:64-75, 2015, doi:10.1016/j.icarus.2014.11.029.
40. Sohl, F., "Revealing Titan's Interior," *Science* 327(5971):1338-1339, 2010, doi:10.1126/science.1186255.
41. Fortes, A.D., "Titan's Internal Structure and the Evolutionary Consequences," *Planetary and Space Science* 60(1):10-17, 2012, doi:10.1016/j.pss.2011.04.010.
42. Tobie, G., Lunine, J.I., and Sotin, C., "Episodic Outgassing as the Origin of Atmospheric Methane on Titan," *Nature* 440(7080):61-64, 2006, doi:10.1038/nature04497.
43. Sohl, F., Hussmann, H., Schwentker, B., Spohn, T. et al., "Interior Structure Models and Tidal Love Numbers of Titan," *Journal of Geophysical Research: Planets* 108(E12):5130, 2003, doi:10.1029/2003je002044.
44. Fortes, A.D., Grindrod, P.M., Trickett, S.K., and Vočadlo, L., "Ammonium Sulfate on Titan: Possible Origin and Role in Cryovolcanism," *Icarus* 188(1):139-153, 2007, doi:10.1016/j.icarus.2006.11.002.
45. Béghin, C., Sotin, C., and Hamelin, M., "Titan's Native Ocean Revealed beneath Some 45 km of Ice by a Schumann-Like Resonance," *Comptes Rendus Géoscience* 342(6):425-433, 2010, doi:10.1016/j.crte.2010.03.003.
46. Nimmo, F. and Bills, B.G., "Shell Thickness Variations and the Long-Wavelength Topography of Titan," *Icarus* 208(2):896-904, 2010, doi:10.1016/j.icarus.2010.02.020.
47. Moore, J.M. and Pappalardo, R.T., "Titan: An Exogenic World?" *Icarus* 212(2):790-806, 2011, doi:10.1016/j.icarus.2011.01.019.
48. Iess, L., Jacobson, R.A., Ducci, M., Stevenson, D.J. et al., "The Tides of Titan," *Science* 337(6093):457-459, 2012, doi:10.1126/science.1219631.
49. Mitri, G., Bland, M.T., Showman, A.P., Radebaugh, J. et al., "Mountains on Titan: Modeling and Observations," *Journal of Geophysical Research: Planets* 115(E10):E10002, 2010, doi:10.1029/2010JE003592.
50. Tobie, G., Grasset, O., Lunine, J.I., Mocquet, A. et al., "Titan's Internal Structure Inferred from a Coupled Thermal-Orbital Model," *Icarus* 175(2):496-502, 2005, doi:10.1016/j.icarus.2004.12.007.
51. Bills, B.G. and Nimmo, F., "Rotational Dynamics and Internal Structure of Titan," *Icarus* 214(1):351-355, 2011, doi:10.1016/j.icarus.2011.04.028.
52. Hemingway, D., Nimmo, F., Zebker, H., and Iess, L., "A Rigid and Weathered Ice Shell on Titan," *Nature* 500(7464):550-552, 2013, doi:10.1038/nature12400.
53. Marion, G.M., Kargel, J.S., Catling, D.C., and Lunine, J.I., "Modeling Ammonia-Ammonium Aqueous Chemistries in the Solar System's Icy Bodies," *Icarus* 220(2):932-946, 2012, doi:10.1016/j.icarus.2012.06.016.
54. Boehler, R., "Temperatures in the Earth's Core from Melting-Point Measurements of Iron at High Static Pressures," *Nature* 363(6429):534-536, 1993, doi:10.1038/363534a0.
55. Barriol, Y., Glaser, K.S., Pop, J., Bartman, B. et al., "The Pressures of Drilling and Production," *Oilfield Review* 17(3):22-41, 2005.

56. Zubrin, R. and Wagner, R., *The Case for Mars: The Plan to Settle the Red Planet and Why We Must*, (New York, Free Press, 1996), ISBN:978-0684835501.
57. Porco, C.C., Baker, E., Barbara, J., Beurle, K. et al., "Imaging of Titan from the Cassini Spacecraft," *Nature* 434(7030):159-168, 2005, doi:10.1038/nature03436.
58. Bird, M.K., Allison, M., Asmar, S.W., Atkinson, D.H. et al., "The Vertical Profile of Winds on Titan," *Nature* 438(7069):800-802, 2005, doi:10.1038/nature04060.
59. Burr, D.M., Bridges, N.T., Marshall, J.R., Smith, J.K. et al., "Higher-Than-Predicted Saltation Threshold Wind Speeds on Titan," *Nature* 517(7532):60-63, 2015, doi:10.1038/nature14088.
60. Manwell, J.F., McGowan, J.G., and Rogers, A.L., *Wind Energy Explained: Theory, Design and Application*, Second Edition, (West Sussex, UK, John Wiley & Sons, 2009), ISBN:978-0470015001.
61. Guo, Y., Keller, J., and LaCava, W., "Combined Effects of Gravity, Bending Moment, Bearing Clearance, and Input Torque on Wind Turbine Planetary Gear Load Sharing: Preprint," To be presented *American Gear Manufacturers Association (AGMA) Fall Technical Meeting*, Dearborn, MI, Oct. 28-30, 2012, National Renewable Energy Laboratory (NREL/CP-5000-55968), Golden, CO.
62. Kumar, V., Paraschivoiu, M., and Paraschivoiu, I., "Low Reynolds Number Vertical Axis Wind Turbine for Mars," *Wind Engineering* 34(4):461-476, 2010, doi:10.1260/0309-524X.3.4.461.
63. Lebonnois, S., Burgalat, J., Rannou, P., and Charnay, B., "Titan Global Climate Model: A New 3-Dimensional Version of the IPSL Titan GCM," *Icarus* 218(1):707-722, 2012, doi:10.1016/j.icarus.2011.11.032.
64. Burr, D.M., Bridges, N.T., Smith, J.K., Marshall, J.R. et al., "The Titan Wind Tunnel: A New Tool for Investigating Extraterrestrial Aeolian Environments," *Aeolian Research* 18:205-214, 2015, doi:10.1016/j.aeolia.2015.07.008.
65. Béghin, C., Simões, F., Krasnoselskikh, V., Schwingenschuh, K. et al., "A Schumann-Like Resonance on Titan Driven by Saturn's Magnetosphere Possibly Revealed by the Huygens Probe," *Icarus* 191(1):251-266, 2007, doi:10.1016/j.icarus.2007.04.005.
66. Choukroun, M. and Grasset, O., "Thermodynamic Data and Modeling of the Water and Ammonia-Water Phase Diagrams up to 2.2 GPa for Planetary Geophysics," *The Journal of Chemical Physics* 133(14):144502, 2010, doi:10.1063/1.3487520.
67. Hanada, N., Hino, S., Ichikawa, T., Suzuki, H. et al., "Hydrogen Generation by Electrolysis of Liquid Ammonia," *Chemical Communications* 46(41):7775-7777, 2010, doi:10.1039/c0cc01982h.
68. Allagui, A., Brazeau, N., Alawadhi, H., Al-momani, F. et al., "Cathodic Contact Glow Discharge Electrolysis for the Degradation of Liquid Ammonia Solutions," *Plasma Processes and Polymers* 12(1):25-31, 2015, doi:10.1002/ppap.201400049.
69. Hickling, A. and Newns, G.R., "1024. Glow-Discharge Electrolysis. Part IV. The Formation of Hydrazine in Liquid Ammonia," *Journal of the Chemical Society (Resumed)* (0):5177-5185, 1961, doi:10.1039/jr9610005177.
70. Hickling, A. and Newns, G.R., "1025. Glow-Discharge Electrolysis. Part V. The Contact Glow-Discharge Electrolysis of Liquid Ammonia," *Journal of the Chemical Society (Resumed)* (0):5186-5191, 1961, doi:10.1039/jr9610005186.
71. Mazzocchin, G.A., Magno, F., and Bontempelli, G., "Glow Discharge Electrolysis on Ammonia in Aqueous Solution," *Journal of Electroanalytical Chemistry and Interfacial Electrochemistry* 45(3):471-482, 1973, doi:10.1016/S0022-0728(73)80058-0.
72. Todd, D., Schwager, M., and Mérida, W., "Thermodynamics of High-Temperature, High-Pressure Water Electrolysis," *Journal of Power Sources* 269:424-429, 2014, doi:10.1016/j.jpowsour.2014.06.144.
73. Reeves, T.G., "Nitrogen Removal: A Literature Review," *Journal (Water Pollution Control Federation)* 44(10):1895-1908, 1972, doi:www.jstor.org/stable/25037627.
74. Environmental Protection Agency, "Wastewater Technology Fact Sheet: Ammonia Stripping," Report # EPA 832-F-00-019, Environmental Protection Agency, Washington, DC, 2000.
75. Onda, K., Kyakuno, T., Hattori, K., and Ito, K., "Prediction of Production Power for High-Pressure Hydrogen by High-Pressure Water Electrolysis," *Journal of Power Sources* 132(1-2):64-70, 2004, doi:10.1016/j.jpowsour.2004.01.046.

76. Laoun, B., "Thermodynamics Aspect of High Pressure Hydrogen Production by Water Electrolysis," *Revue des Energies Renouvelables* 10(3):435-444, 2007.
77. LeRoy, R.L., Bowen, C.T., and LeRoy, D.J., "The Thermodynamics of Aqueous Water Electrolysis," *Journal of the Electrochemical Society* 127(9):1954-1962, 1980, doi:10.1149/1.2130044.
78. National Institute of Standards and Technology, "NIST Reference Fluid Thermodynamic and Transport Properties Databse (Refprop): Version 9.1," 2014.
79. Isaac, F.S. and John, W.C., "Metallic Hydrogen: The Most Powerful Rocket Fuel Yet to Exist," *Journal of Physics: Conference Series* 215(1):012194, 2010, doi:10.1088/1742-6596/215/1/012194.
80. Sutton, G.P. and Biblarz, O., *Rocket Propulsion Elements*, (Hoboken, NJ, John Wiley & Sons, Inc., 2010), ISBN:978-0470080245.
81. Lewis, J.S., "Space Resources,"in G.D. Considine and P.H. Kulik (Eds.), *Van Nostrand's Scientific Encyclopedia* (Hoboken, NJ, John Wiley & Sons, Inc., 2005), doi:10.1002/0471743984.vse8672.
82. SpaceX, "Falcon Heavy," 2016, [cited Dec. 19, 2016], http://www.spacex.com/falcon-heavy.
83. Spaceflight101.com, "Falcon Heavy," 2016, [cited Dec. 19, 2016], http://spaceflight101.com/spacerockets/falcon-heavy/.
84. Kass, M., Noakes, M., Kaul, B., Edwards, D. et al., "Experimental Evaluation of a 4-cc Glow-Ignition Single-Cylinder Two-Stroke Engine," SAE Technical Paper 2014-01-1673, 2014, doi:10.4271/2014-01-1673.
85. Baland, R.-M., Tobie, G., Lefèvre, A., and Hoolst, T.V., "Titan's Internal Structure Inferred from Its Gravity Field, Shape, and Rotation State," *Icarus* 237(Supplement C):29-41, 2014, doi:10.1016/j.icarus.2014.04.007.
86. Zhao, F., Assanis, D., Asmus, T., Dec, J. et al., *Homogeneous Charge Compression Ignition (HCCI) Engines: Key Research and Development Issues*, (Warrendale, Society of Automotive Engineers, Inc., 2003), ISBN:978-0-7680-1123-4.
87. Cecrle, E., Depcik, C., Guo, J., and Peltier, E., "Analysis of the Effects of Reformate (Hydrogen/Carbon Monoxide) as an Assistive Fuel on the Performance and Emissions of Used Canola-Oil Biodiesel," *International Journal of Hydrogen Energy* 37(4):3510-3527, 2012, doi:10.1016/j.ijhydene.2011.11.026.
88. Mathurkar, H., "Minimum Ignition Energy and Ignition Probability for Methane, Hydrogen and Their Mixtures," Ph.D. thesis, Chemical Engineering, Loughborough University, Loughborough, 2009.
89. Yap, D., Megaritis, A., Peucheret, S., Wyszynski, M. et al., "Effect of Hydrogen Addition on Natural Gas HCCI Combustion," SAE Technical Paper 2004-01-1972, 2004, doi:10.4271/2004-01-1972.
90. Yap, D., Peucheret, S.M., Megaritis, A., Wyszynski, M.L. et al., "Natural Gas HCCI Engine Operation with Exhaust Gas Fuel Reforming," *International Journal of Hydrogen Energy* 31(5):587-595, 2006, doi:10.1016/j.ijhydene.2005.06.002.
91. Zhang, Z., Xie, Q., Liang, J., and Li, G., "Numerical Study of Combustion Characteristics of a Natural Gas HCCI Engine with Closed Loop Exhaust-Gas Fuel Reforming," *Applied Thermal Engineering* 119(Supplement C):430-437, 2017, doi:10.1016/j.applthermaleng.2017.03.079.
92. Schefer, R.W., Wicksall, D.M., and Agrawal, A.K., "Combustion of Hydrogen-Enriched Methane in a Lean Premixed Swirl-Stabilized Burner," *Proceedings of the Combustion Institute* 29(1):843-851, 2002, doi:10.1016/S1540-7489(02)80108-0.
93. Dimitrov, V. and Bar-Nun, A., "Kinetic Pathways in the Atmospheric Chemistry of Titan - A Generalized Analysis," *Progress in Reaction Kinetics and Mechanism* 29(1):299-420, 2004, doi:10.3184/007967404323147058.
94. Kee, R.J., Rupley, F.M., Meeks, E., and Miller, J.A., "Chemkin-III: A Fortran Chemical Kinetics Package for the Analysis of Gas-Phase Chemical and Plasma Kinetics," Sandia National Laboratories, 1996.
95. Chen, R. and Milovanovic, N., "A Computational Study into the Effect of Exhaust Gas Recycling on Homogeneous Charge Compression Ignition Combustion in Internal

Combustion Engines Fuelled with Methane," *International Journal of Thermal Sciences* 41(9):805-813, 2002, doi:10.1016/S1290-0729(02)01375-3.

96. Srinivasan, K.K., Krishnan, S.R., Qi, Y., Midkiff, K.C. et al., "Analysis of Diesel Pilot-Ignited Natural Gas Low-Temperature Combustion with Hot Exhaust Gas Recirculation," *Combustion Science and Technology* 179(9):1737-1776, 2007, doi:10.1080/00102200701259882.
97. Zheng, J. and Caton, J.A., "Effects of Operating Parameters on Nitrogen Oxides Emissions for a Natural Gas Fueled Homogeneous Charged Compression Ignition Engine (HCCI): Results from a Thermodynamic Model with Detailed Chemistry," *Applied Energy* 92:386-394, 2012, doi:10.1016/j.apenergy.2011.11.025.
98. Kawasaki, K., Takegoshi, A., Yamane, K., Ohtsubo, H. et al., "An Experimental Study on the Improvement of Engine Performance and Exhaust Emissions from Small-Scale PCCI Engines Fuelled by Natural Gas," SAE Technical Paper 2005-01-2124, 2005, doi:10.4271/2005-01-2124.
99. Kawasaki, K., Takegoshi, A., Yamane, K., Ohtsubo, H. et al., "Combustion Improvement and Control for a Natural Gas HCCI Engine by the Internal EGR by Means of Intake-Valve Pilot-Opening," SAE Technical Paper 2006-01-0208, 2006, doi:10.4271/2006-01-0208.
100. Kuzuyama, H., Machida, M., Akihama, K., Inagaki, K. et al., "A Study on Natural Gas Fueled Homogeneous Charge Compression Ignition Engine - Expanding the Operating Range and Combustion Mode Switching," SAE Technical Paper 2007-01-0176, 2007, doi:10.4271/2007-01-0176.
101. Stanglmaier, R. and Roberts, C., "Homogeneous Charge Compression Ignition (HCCI): Benefits, Compromises, and Future Engine Applications," SAE Technical Paper 1999-01-3682, 1999, doi:10.4271/1999-01-3682.
102. Mørch, C.S., Bjerre, A., Gøttrup, M.P., Sorenson, S.C. et al., "Ammonia/Hydrogen Mixtures in an Si-Engine: Engine Performance and Analysis of a Proposed Fuel System," *Fuel* 90(2):854-864, 2011, doi:10.1016/j.fuel.2010.09.042.
103. Sprouse, C. III and Depcik, C., "Review of Organic Rankine Cycles for Internal Combustion Engine Exhaust Waste Heat Recovery," *Applied Thermal Engineering* 51(1-2):711-722, 2013, doi:10.1016/j.applthermaleng.2012.10.017.
104. Tate, K., "International Space Station's Cooling System: How It Works (Infographic)," 2013, http://www.space.com/21059-space-station-cooling-system-explained-infographic.html, accessed May 31, 2016.
105. Miyahara, K., "N_2-Hydrogenation on Solid Surface with Glow Discharge," *Chemistry Letters* 13(6):849-852, 1984, doi:10.1246/cl.1984.849.
106. Heywood, J.B., *Internal Combustion Engine Fundamentals*, (New York, McGraw-Hill, Inc., 1988), ISBN:978-0070286375.
107. Depcik, C., Mangus, M., and Ragone, C., "Ozone-Assisted Combustion-Part I: Literature Review and Kinetic Study Using Detailed N-Heptane Kinetic Mechanism," *Journal of Engineering for Gas Turbines and Power* 136(9):091507-091507, 2014, doi:10.1115/1.4027068.
108. Hindmarsh, A.C., "Serial Fortran Solvers for Ode Initial Value Problems [Internet]," Lawrence Livermore National Laboratory, Aug. 5, 2002, [cited Apr. 18, 2006], http://www.llnl.gov/CASC/odepack/.
109. Smith, G.P., Golden, D.M., Frenklach, M., Moriarty, N.W. et al., "Gri-Mech 3.0," 2008, [cited Sept. 7, 2008], http://www.me.berkeley.edu/gri_mech/.
110. Zhang, Y., Huang, Z., Wei, L., and Niu, S., "Experimental and Kinetic Study on Ignition Delay Times of Methane/Hydrogen/Oxygen/Nitrogen Mixtures by Shock Tube," *Chinese Science Bulletin* 56(26):2853-2861, 2011, doi:10.1007/s11434-011-4635-4.
111. Bramlette, R., "Development, Modeling, Simulation, and Testing of a Novel Propane-Fueled Brayton-Gluhareff Cycle Acoustically-Pressurized Ramjet Engine," Mechanical Engineering, University of Kansas, Lawrence, 2016.
112. UCSD, "Chemical-Kinetic Mechanisms for Combustion Applications," Mechanical and Aerospace Engineering (Combustion Research) Referenced, 2014, http://web.eng.ucsd.edu/mae/groups/combustion/mechanism.html, accessed May 31, 2016.

113. Depcik, C., Jacobs, T., Hagena, J., and Assanis, D., "Instructional Use of a Single-Zone, Pre-Mixed Spark-Ignition Heat Release Simulation," *International Journal of Mechanical Engineering Education* 35(1):1-31, 2007, doi:10.7227/IJMEE.35.1.1.

114. Soyhan, H.S., Yasar, H., Walmsley, H., Head, B. et al., "Evaluation of Heat Transfer Correlations for HCCI Engine Modeling," *Applied Thermal Engineering* 29(2-3):541-549, 2009, doi:10.1016/j.applthermaleng.2008.03.014.

115. Mattson, J., Mangus, M., and Depcik, C., "Efficiency and Emissions Mapping for a Single-Cylinder, Direct Injected Compression Ignition Engine," SAE Technical Paper 2014-01-1242, 2014, doi:10.4271/2014-01-1242.

116. Lavoie, G.A., Ortiz-Soto, E., Babajimopoulos, A., Martz, J.B. et al., "Thermodynamic Sweet Spot for High-Efficiency, Dilute, Boosted Gasoline Engines," *International Journal of Engine Research* 14(3):260-278, 2012, doi:10.1177/1468087412455372.

117. Kar, K., Roberts, S., Stone, R., Oldfield, M. et al., "Instantaneous Exhaust Temperature Measurements Using Thermocouple Compensation Techniques," SAE Technical Paper 2004-01-1418, 2004, doi:10.4271/2004-01-1418.

118. Langness, C., Mangus, M., and Depcik, C., "Construction, Instrumentation, and Implementation of a Low Cost, Single-Cylinder Compression Ignition Engine Test Cell," SAE Technical Paper 2014-01-0817, 2014, doi:10.4271/2014-01-0817.

119. Li, C., "Piston Thermal Deformation and Friction Considerations," SAE Technical Paper 820086, 1982, doi:10.4271/820086.

120. Enomoto, Y., Aoki, Y., Emi, M., and Kimura, S., "Heat Transfer Coefficient on the Combustion Chamber Wall Surfaces in a Naturally Aspirated Direct-Injection Diesel Engine," *International Journal of Engine Research* 15(5):606-625, 2014, doi:10.1177/1468087413500060.

121. Maurya, R.K. and Agarwal, A.K., "Experimental Investigation on the Effect of Intake Air Temperature and Air-Fuel Ratio on Cycle-to-Cycle Variations of HCCI Combustion and Performance Parameters," *Applied Energy* 88(4):1153-1163, 2011, doi:10.1016/j.apenergy.2010.09.027.

122. Gomes Antunes, J.M., Mikalsen, R., and Roskilly, A.P., "An Investigation of Hydrogen-Fuelled HCCI Engine Performance and Operation," *International Journal of Hydrogen Energy* 33(20):5823-5828, 2008, doi:10.1016/j.ijhydene.2008.07.121.

123. Singh, G., Singh, A.P., and Agarwal, A.K., "Experimental Investigations of Combustion, Performance and Emission Characterization of Biodiesel Fuelled HCCI Engine Using External Mixture Formation Technique," *Sustainable Energy Technologies and Assessments* 6:116-128, 2014, doi:10.1016/j.seta.2014.01.002.

124. Bhaduri, S., Berger, B., Pochet, M., Jeanmart, H. et al., "HCCI Engine Operated with Unscrubbed Biomass Syngas," *Fuel Processing Technology* 157:52-58, 2017, doi:10.1016/j.fuproc.2016.10.011.

125. Catapano, F., Di Iorio, S., Magno, A., Sementa, P. et al., "A Comprehensive Analysis of the Effect of Ethanol, Methane and Methane-Hydrogen Blend on the Combustion Process in a PFI (Port Fuel Injection) Engine," *Energy* 88:101-110, 2015, doi:10.1016/j.energy.2015.02.051.

126. Siporin, S.E. and Davis, R.J., "Use of Kinetic Models to Explore the Role of Base Promoters on Ru/MgO Ammonia Synthesis Catalysts," *Journal of Catalysis* 225(2):359-368, 2004, doi:10.1016/j.jcat.2004.03.046.

127. Lunsford, J.H., "Catalytic Conversion of Methane to More Useful Chemicals and Fuels: A Challenge for the 21st Century," *Catalysis Today* 63(2):165-174, 2000, doi:10.1016/S0920-5861(00)00456-9.

128. Beech, M., *Terraforming: The Creating of Habitable Worlds*, (New York, Springer Science & Business Media, 2009), ISBN:978-0-387-09795-4.

129. Dole, S.H., *Habitable Planets for Man*, (New York, RAND Corporation, 2007), ISBN:9780833042279.

Appendix

FIGURE 1 Theoretical energy generation system on the surface of Titan.